

Prediction of Ligand Binding Affinity by the Combination of Replica-Exchange Method and Double-Decoupling Method

Yuko Okamoto,^{*,†,‡,§,||,#} Hironori Kokubo,^{⊥,#} and Toshimasa Tanaka[⊥]

[†]Department of Physics, Graduate School of Science, Nagoya University, Furo-cho, Chikusa-ku, Nagoya, Aichi 464-8602, Japan

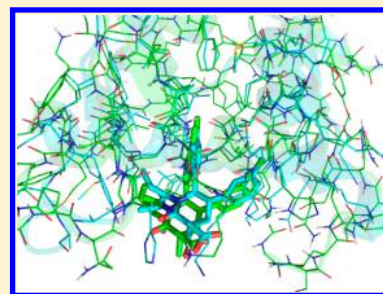
[‡]Structural Biology Research Center, Graduate School of Science, Nagoya University, Furo-cho, Chikusa-ku, Nagoya, Aichi 464-8602, Japan

[§]Center for Computational Science, Graduate School of Engineering, Nagoya University, Furo-cho, Chikusa-ku, Nagoya, Aichi 464-8603, Japan

^{||}Information Technology Center, Nagoya University, Furo-cho, Chikusa-ku, Nagoya, Aichi 464-8601, Japan

[⊥]Medicinal Chemistry Research Laboratories, Pharmaceutical Research Division, Takeda Pharmaceutical Co., Ltd., 26-1 Muraoka-Higashi 2-chome, Fujisawa, Kanagawa 251-8585, Japan

ABSTRACT: A prediction method for ligand binding affinities to proteins is proposed. We first predict the structures of protein–ligand complex by the replica-exchange umbrella sampling or its extension. We then calculate ligand binding affinities based on these predicted ligand–protein bound structures by the double-decoupling method. As a test of the effectiveness of the proposed method, we applied it to the system of the oncoprotein MDM2 and a ligand. The value of the predicted binding affinity turned out to be in good agreement with that from experiments.



1. INTRODUCTION

Free energy plays an important role in many chemical processes.^{1–11} In order to obtain free energy computationally, molecular simulation techniques are commonly used. For drug design, in particular, the double-decoupling method (DDM)⁵ is one of effective methods for calculations of absolute protein–ligand binding affinity. However, the accurate knowledge of ligand–protein bound structures is required for the application of DDM,^{9,10} which often relies on experiments or docking software such as GOLD.¹² The docking software may succeed in predicting the protein–ligand binding structures; however, they often cannot be directly used for protein–ligand affinity calculations. In previous works, we therefore developed a prediction method^{13,14} for ligand–protein bound structures based on the replica-exchange umbrella sampling method (REUS)¹⁵ and one¹⁶ based on the 2-dimensional replica-exchange method (REUS/REST) that combines REUS and replica-exchange with solute tempering (REST).¹⁷ Although the former method can already predict ligand–protein bound structures accurately, the latter one allows the ligand to go in and come out of the binding pocket of a protein many more times than the former during a single simulation run, which will give more accurate free energy. However, the latter is more computationally demanding than the former. Provided that we have sufficient computational power, we want to use the latter method. We therefore propose a prediction method for ligand binding affinities to proteins as follows. We first predict the protein–ligand binding structure by either REUS or REUS/

REST simulation. Using the predicted protein–ligand binding structure, we then calculate ligand binding affinity by DDM.

As a test of the effectiveness of our method, we applied the REUS/REST approach to a protein–ligand system, MDM2 (Protein Data Bank (PDB)¹⁸ ID: 1T4E for receptor conformation and 4ERF for a ligand) and obtained the predicted ligand binding mode. MDM2 has a ubiquitin ligase activity and targets tumor protein p53. Using the predicted structure, we then performed the absolute binding free energy calculation by DDM.

The article is organized as follows. Section 2 summarizes our methods. In section 3, the computational details are provided. Section 4 gives the results and discussion about the application of our method to a protein–ligand system. We devote section 5 to conclusions.

2. METHODS

Two-Dimensional Replica-Exchange Method: REUS/REST. Because our method for predicting ligand–protein bound structures by the two-dimensional replica-exchange method REUS/REST is explained in detail elsewhere,¹⁶ here, we give only essential parts for completeness.

The original potential energy of the system of N atoms with coordinates $q = (q_1, \dots, q_N)$ can be written as

$$E(q) = U_H(q) + U_S(q) + U_{ss}(q) \quad (1)$$

Received: April 9, 2014

Published: June 25, 2014

where the first, the second, and the third terms on the right-hand side represent the intramolecular interactions within the ligand, those between ligand atoms and protein–water atoms, and those between atoms in the protein and solvent, respectively. The subscript l represents ligand and s protein/water. We introduce REUS and REST as a two-dimensional replica-exchange method by modifying the original potential energy as follows. We consider M ($=M_1M_2$) noninteracting replicas of the original system. We have the following total potential energy for the i -th replica having coordinates $q^{[i]}$:

$$E_{m_1, m_2}(q^{[i]}) = \frac{\beta_{m_2}}{\beta_0} U_l(q^{[i]}) + \sqrt{\frac{\beta_{m_2}}{\beta_0}} U_{ls}(q^{[i]}) + U_{ss}(q^{[i]}) + V_{m_1}(q^{[i]}) \quad (2)$$

where $\beta_{m_2}/\beta_0 (= \gamma_{m_2})$ are the REST scaling parameters ($m_2 = 1, \dots, M_2$), and the last term in eq 2 is the umbrella potential defined by

$$V_{m_1}(q) = k_{m_1}(\xi(q) - d_{m_1})^2, \quad (m_1 = 1, \dots, M_1) \quad (3)$$

where the reaction coordinate ξ stands for the distance between the binding site and the ligand, d_{m_1} is the midpoint distance, and k_{m_1} is the strength of the umbrella potentials. REUS performs a random walk in the reaction coordinate ξ , and REST performs a random walk in parameter γ so that interactions between ligand atoms and other atoms are weakened as γ gets small.

Protocol for the Prediction of a Protein–Ligand Binding Structure. Our protocol is as follows. In the first step, we determine the force-field parameters such as charges for the ligand molecule.¹⁹ Next, we put a protein (without a ligand) in a solvation box and perform the REUS/REST simulation. Note that we need knowledge of the ligand binding site for our simulations. The binding site is, however, often known by experiments or by short simulations. If there are more than one possible binding sites, multiple independent REUS/REST simulations should be performed for each binding site.

In the second step, from the results of the REUS/REST simulation, we obtain the value of ξ that corresponds to the global minimum in potential of mean force (PMF). Although the weighted histogram analysis method²⁰ is equally useful, here, we use the multistate Bennett acceptance ratio estimator (MBAR)²¹ to obtain the canonical distributions and PMF.

In the third step, we predict the ligand–protein bound structures by the principal component analysis (PCA).^{22–27} As the predicted binding structure, we select a typical structure that exists in the global-minimum free energy state on the free energy landscape with respect to the first and second principal component axes.

Calculation of a Protein–Ligand Binding Free Energy.

Double-decoupling method (DDM) is used to calculate absolute binding free energy. In DDM, because of the thermodynamic cycle relation, the binding free energy (affinity) can be calculated by subtracting the solvation free energy of a ligand in water from that of a ligand binding to a protein with a positional constraint and adding the reweighting term for the constraint and standard state corrections. The thermodynamic integration method (TI)¹ can be applied to the calculation of the binding affinity. We consider two systems: the ligand in water and the protein–ligand complex in water. We calculate the electrostatic and Lennard-Jones (vdW) free energy separately. We can introduce a parameter λ , and the potential

energy involving the ligand atoms, for the electrostatic interactions, is given by

$$U(\lambda) = (1 - \lambda)U_0 + \lambda U_1 \quad (14)$$

where U_0 is the potential energy of the system in which the ligand does not interact with the surrounding atoms electrostatically and U_1 is for the original interaction. For the vdW interactions of the ligand atoms with the surrounding, we have the following softcore potential:

$$U(\lambda) = 4\epsilon\lambda \left(\frac{1}{[\alpha(1 - \lambda) + (r/\sigma)^6]^2} - \frac{1}{\alpha(1 - \lambda) + (r/\sigma)^6} \right) \quad (15)$$

where $\lambda = 0$ corresponds to the case where the ligand does not have any interactions with the surrounding atoms and $\lambda = 1$ corresponds to the case where the ligand does not have electrostatic interactions but have full vdW interactions with the surrounding atoms.

The solvation free energy for the two systems can be separately calculated by the following equation:

$$\Delta G = G_1 - G_0 = \int_0^1 \left\langle \frac{\partial U}{\partial \lambda} \right\rangle_{\lambda} d\lambda \approx \sum_i \left\langle \frac{\partial U}{\partial \lambda} \right\rangle_{\lambda_i} \Delta \lambda_i \quad (16)$$

Here, we use the predicted binding mode obtained by the REUS/REST simulation as the initial structure of DDM simulations. Detailed calculation conditions are shown in the last part of next section.

3. COMPUTATIONAL DETAILS

We studied an oncoprotein MDM2 with a ligand. We selected a compound 29 as a ligand from Protein Data Bank (PDB), 4ERF, and a receptor conformation of PDB ID, 1T4E. Figure 1

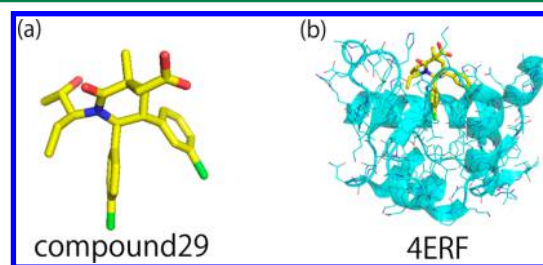


Figure 1. (a) Ligand molecule conformation complexed to a protein (from PDB). (b) Protein–ligand complex structure (PDB ID: 4ERF). The figures were created by PyMOL.

shows the structure of compound 29 and MDM2. Note that we avoided using the receptor conformation from the same PDB for the rigorous investigation of the applicability of our method. This corresponds to so-called “cross docking” examination in the docking software. Thus, our method can be applied to the practical cases where we use a common receptor structure to predict the binding poses of many design ligands.

The charges for the ligand atoms were determined by the RESP method,^{28,29} as explained in detail elsewhere.¹⁹ For the protein we used the AMBER *ff99SB* parameters³⁰ and for water we used the TIP3P parameters.³¹ We remark that the present ligand is negatively charged and that in such a case one

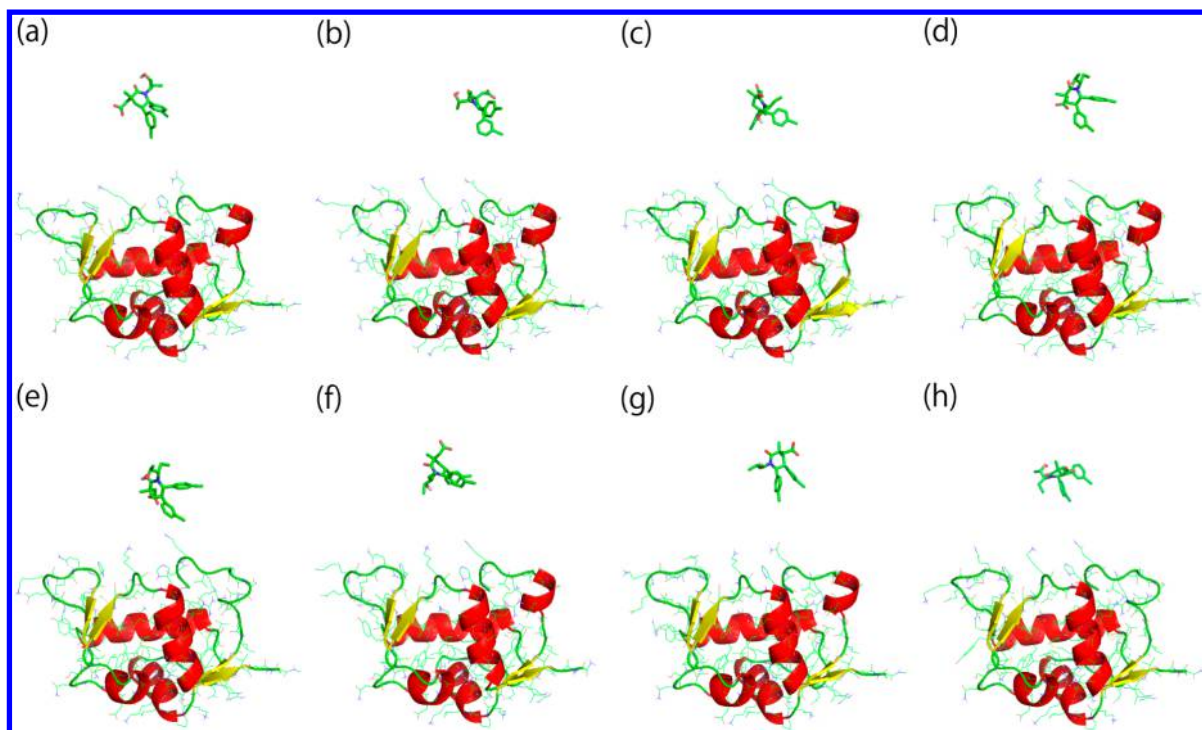


Figure 2. Snapshots of the initial eight structures for the REUS/REST simulations with the largest umbrella potential midpoint value of $d_{m_1} = 25 \text{ \AA}$. The figures were created using PyMOL.

has to be careful about finite-size artifacts in the binding affinity calculations.^{32,33}

Next, we immersed the protein structure of MDM2 from PDB 1T4E without the ligand in a water box with a solvation of at least 12.0 \AA from the protein, and a ligand of PDB 4ERF was placed in an arbitrary solvent region outside the binding pocket. Water molecules overlapped with the ligand were removed. The total number of water molecules was 7229 for the system. The system was neutralized by adding three chloride ions. The periodic boundary conditions were imposed and the particle mesh Ewald method³⁴ was used. The Berendsen thermostat was employed to keep the temperature at $T_0 = 300 \text{ K}$, and the pressure was kept at 1.0 atm by the weak-coupling method.³⁵ The bond lengths involving hydrogen atoms were constrained by the SHAKE method,³⁶ which allowed the time step of 2.0 fs . We fixed the coordinates of the protein heavy atoms that were more than 12 \AA away from the ligand by the harmonic constraints of strength $k = 1.0 \text{ kcal}/(\text{mol \AA}^2)$.

The reaction coordinate ξ for the system was the distance between the center of mass of the ligand and the center of mass of backbone heavy atoms of two arbitrarily selected residues of the protein near the binding site, which were LEU54 and GLN58.

The $M_1 = 24$ midpoint values for the umbrella potentials were $d_{m_1} = 5.0, 5.5, 6.0, 6.5, 7.0, 7.5, 8.0, 8.5, 9.0, 9.5, 10.0, 10.5, 11.0, 12.0, 13.0, 14.0, 15.0, 16.0, 17.5, 19.0, 20.5, 22.0, 23.5$, and 25.0 \AA , and we set $k_{m_1} = 1.0 \text{ kcal}/(\text{mol \AA}^2)$ for $d_{m_1} \leq 13.0 \text{ \AA}$ and $k_{m_1} = 0.5 \text{ kcal}/(\text{mol \AA}^2)$ for $d_{m_1} > 13.0 \text{ \AA}$. The $M_2 = 8$ REST parameters were $\gamma_{m_2} = 0.10, 0.19, 0.27, 0.37, 0.49, 0.63, 0.80$, and 1.00 . The replica exchanges were tried every 0.1 ps for REUS and every 5.0 ps for REST.

Next, we prepared the initial structures of the REUS/REST simulations as follows. We performed the umbrella sampling

equilibration runs for 1.6 ns with the largest midpoint distance ($d_{m_1} = 25 \text{ \AA}$), and eight structures were extracted at even intervals ($0.2, 0.4, 0.6, 0.8, 1.0, 1.2, 1.4, 1.6 \text{ ns}$). Figure 2 shows these eight structures. Starting from the structures in the figure, we continued the simulations from the largest reaction coordinate to the smallest one. That is, the reaction coordinates were gradually decreased by using umbrella potentials with $d_{m_1} = 25 \text{ \AA}$ to those with $d_{m_1} = 5 \text{ \AA}$ for each of the eight structures. The simulations were performed for 100 ps for each umbrella potential, and the obtained $M (= M_1 \times M_2 = 24 \times 8 = 192)$ structures were used as the initial conformations for the 192 replicas of the REUS/REST simulations.

For each replica, the production run was performed for 50 ns , but the data of the first 10 ns were discarded from the analyses. Ten thousand conformations for each midpoint distance of umbrella potentials were collected for the PMF analyses.

In order to obtain the predicted binding structures of ligand molecules from PMF, we extracted conformations which have the reaction coordinates close to the global-minimum PMF (in range $\pm 0.2 \text{ \AA}$) and the unbiased potential energy near the average potential energy (in range $\pm 20.0 \text{ kcal/mol}$), the number of which turned out to be 1837.

Absolute binding free energy calculation by the double-decoupling method (DDM) was performed by using the predicted binding mode. The corresponding restart file with the equilibrated coordinates was extracted from the trajectory. Because the system was already equilibrated, we did not need the equilibration runs before the free energy calculation. DDM consists of the simulation of the ligand in water and the one of the protein–ligand complex in water. The value of α for the softcore potential was set to be 0.5 . We calculated the vdW and electrostatic free energy separately. Eleven points of equally spaced λ values, $0.0, 0.1, 0.2, 0.3, 0.4, 0.5, 0.6, 0.7, 0.8, 0.9$, and

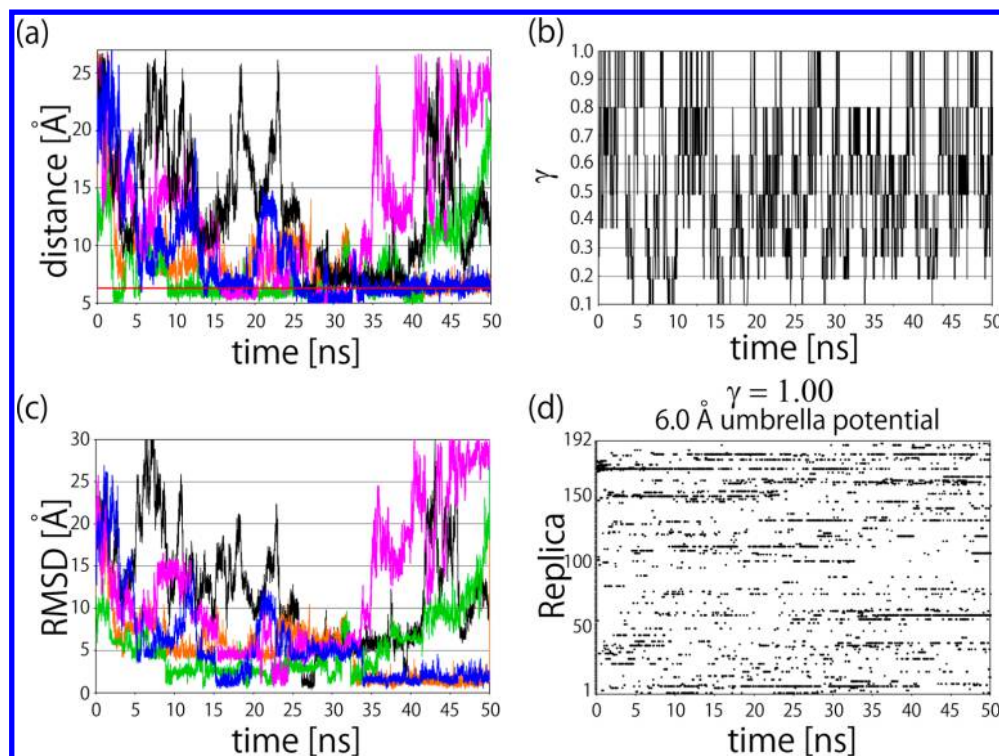


Figure 3. Time series of (a) the reaction coordinate ξ (the distances from the protein pocket), (b) the solute tempering parameter γ , (c) RMSD (in Å) from the correct binding mode (a blue ligand in Figure 6 below), and (d) replica exchange for the third umbrella potential ($k_3 = 1.0$ kcal/(mol Å²) and $d_3 = 6.0$ Å) and the eighth solute tempering parameter with the original interaction ($\gamma = 1$), obtained from the REUS/REST simulation of the 2ERF system. Time series of Replicas 48 (orange), 64 (green), 112 (pink), 140 (black), and 189 (blue) are shown for parts a and c as representatives. The horizontal bold red line at 6.4 Å in part a shows the correct binding distance from PDB.

1.0, were used for the electrostatic part. On the other hand, 33 points unequally spaced λ values were used for the vdW part, because of the shape of $\langle \partial U / \partial \lambda \rangle_\lambda$ by the softcore potential, that is, the interval of 0.02 between 0.0 and 0.36, and that of 0.04 between 0.36 and 1.00 were used. The simple harmonic constraint was used to keep the ligand position while the interactions between the ligand and the system were weakened during the simulation at each λ . A heavy atom of the ligand, which is close to the center of mass of the ligand was harmonically constrained to the reference position of the predicted binding mode with the strength $k = 2.0$ kcal/(mol Å²) (in $k(r - r_0)^2$). The analytic reweighting term, $-k_B T \ln V_{\text{sim}}/V_0 = -k_B T \ln(2\pi k_B T/k)^{3/2}/V_0$, was thus 4.48 kcal/mol. The protein heavy atoms which were more than 12 Å far away from the ligand were also constrained to the reference positions. Here, we assumed that these constrained protein atoms do not contribute to the binding events from the fact that almost all the known PDB structures of MDM2 have essentially very similar structures.

The simulations of length 5.0 ns were performed for the ligand/water system for each λ point for both vdW and electrostatic parts. On the other hand, five independent simulations of length 3.0 ns by assigning different initial velocities were performed for the protein–ligand complex system for each λ point. Longer simulations were performed in total for the complex system than for the ligand/water system because the complex system was more complicated and needed longer simulations for better sampling. Thermodynamic integration (TI) method was used to calculate the free energy. We found that free energy perturbation method (FEP)² and Bennett acceptance ratio method (BAR)³ gave similar values

(the differences of the calculated binding free energy among TI, FEP, and BAR were within 0.23 kcal/mol in this system). We also remark that the present method of dividing vdW and electrostatic parts may depend on path. It was, however, shown that it gave reasonable results for smaller molecular systems,³⁷ and we are following this approach.

4. RESULTS AND DISCUSSION

We now give the simulation results.

Figure 3 shows the reaction coordinate ξ , REST parameters γ root-mean-square distance (RMSD) from the correct binding mode, and replica number as functions of simulation time, which were obtained from our REUS/REST simulation. We observe that most of the quantities oscillated between low values and high ones during the REUS/REST simulation. Because these quantities are supposed to make random walk during the REUS/REST simulation, we consider that the simulation performed properly. Table 1 lists the number of tunneling events during the REUS/REST simulation. The

Table 1. Number of Tunneling Events of the System Examined in the Present Study

	4ERF ^a
from min to max	79
from max to min	62
either direction	141
return	39

^a4ERF: Protein Data Bank ID of the system. The details of the definition are given elsewhere.¹⁶

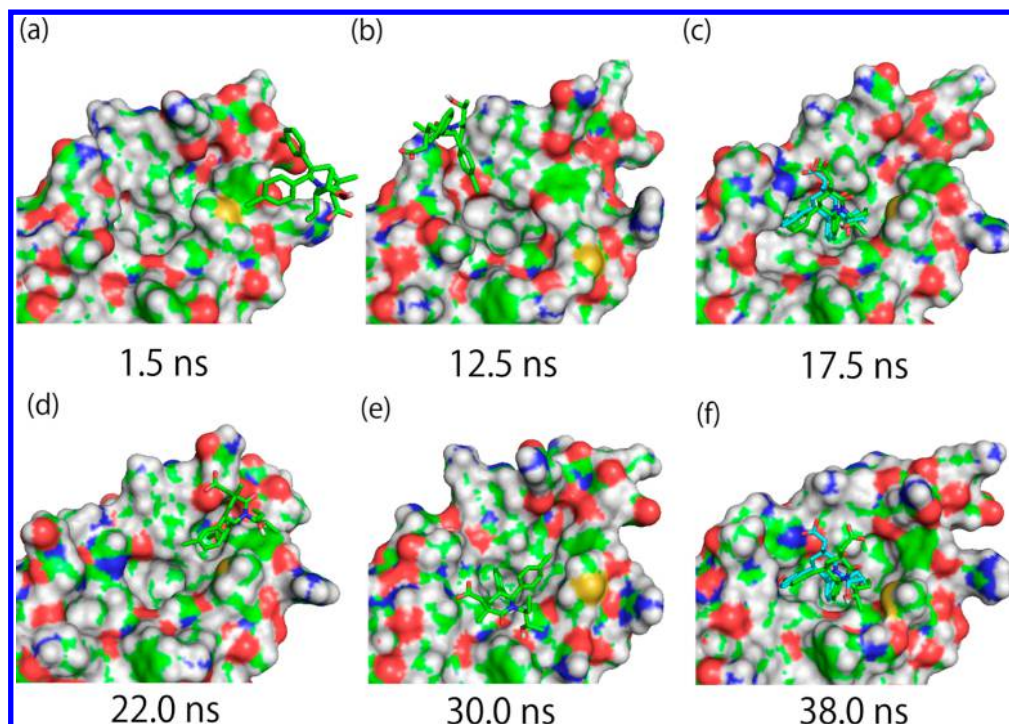


Figure 4. Typical snapshots from the REUS/REST simulation for Replica 189 for the 4ERF system. The configurations were taken at (a) 1.5 ns, (b) 12.5 ns, (c) 17.5 ns, (d) 22.0 ns, (e) 30.0 ns, and (f) 38.0 ns. The RMSD from the correct ligand binding mode from PDB (4ERF) is (a) 24.4 Å, (b) 14.0 Å, (c) 1.1 Å, (d) 11.4 Å, (e) 6.6 Å, and (f) 2.3 Å. In c and f, the PDB conformation of the ligand (blue) was superimposed. The figures were created using PyMOL.

ligand tends to get trapped in states of energy local minima, when it is in the min region (ξ is about 6 Å). Thus, a large number of tunneling events implies that the conformational sampling is good. We again consider that the simulation performed properly.

In Figure 4, typical snapshots from the REUS/REST simulation for one of the replicas (Replica 189) are shown. The ligand approached the pocket from a to c where good agreement of binding structure with experimental one was attained. The ligand then went out of the pocket and came back from d to f through replica exchange. We see that the protein pocket changed the conformations largely during the simulation, which implies the “induced-fit.” These snapshots are consistent with what we observed in Figure 3a and c (see the blue curves in the Figures for the corresponding replica).

Figure 5 shows the PMF $W_{\lambda=\{0\}}(\xi)$ for the system that was obtained by applying the MBAR reweighting techniques to the data from the REUS/REST simulation. The vertical dotted lines show the correct binding distance from PDB. We see that the REUS/REST simulation could detect the correct binding distance as the global minimum in PMF.

In Figure 6, we compare the experimental binding mode (blue) from PDB with the predicted one. We see that they are in good agreement when the fluctuations of the protein and ligand structures are taken into account. We quantified the agreement of the predicted ligand structure with the one of PDB in Figure 6. We first superimposed the coordinates of both structures with respect to all the protein C α atoms by translation and rotation. We then calculated the RMSD of the two ligand structures without translation and rotation. The calculated RMSD value was 1.37 Å. We think that the predicted binding mode is essentially the same, considering the apparent translation of the atoms around the pockets. We also calculated

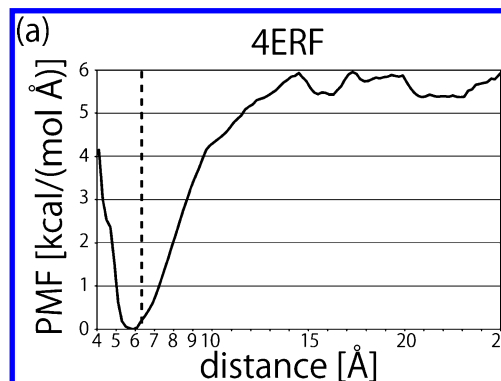


Figure 5. Potential of mean force profile along the reaction coordinate ξ (the distance from the protein pocket) for the system 4ERF. The vertical dotted line shows the distance of the experimental structure from PDB: 6.4 Å.

the RMSD value of the ligand conformation after the superposition by translation and rotation, in order to examine the difference of the ligand internal conformations, which was 0.68 Å. The ligand internal conformation was indeed very similar.

In Figure 7, $\langle \partial U / \partial \lambda \rangle_\lambda$ are plotted as functions of λ for the electrostatic and vdW free energy calculations. The curve of $\langle \partial U / \partial \lambda \rangle_\lambda$ as functions of λ of the vdW free energy calculations is sharply peaked, suggesting the necessity of sufficient λ points. On the other hand, the near linearity of the electrostatic $\langle \partial U / \partial \lambda \rangle_\lambda$ as functions of λ indicates that smaller number of λ points would be sufficient compared to the vdW calculation. The shapes of $\langle \partial U / \partial \lambda \rangle_\lambda$ should be smooth after the convergence. We calculated the absolute binding free energy by integrating these plots.

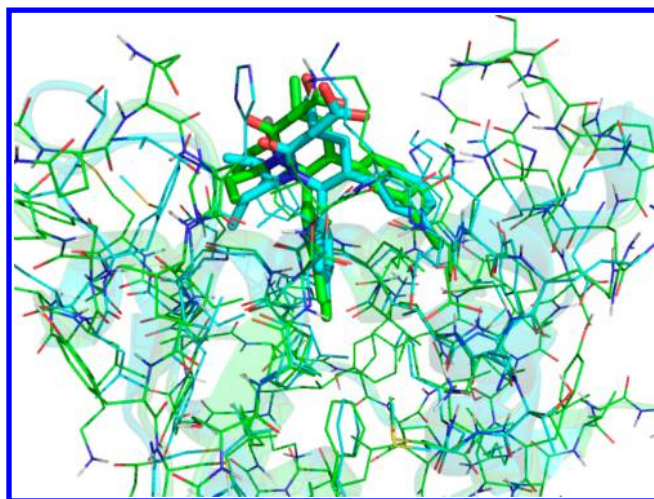


Figure 6. Comparison of the predicted binding mode by the REUS/REST simulation (green) with the experimental ligand binding mode from PDB (blue). The figure was created using PyMOL.

Table 2 lists the results of the absolute binding free energy calculations. We see that this ligand mainly binds by the vdW interactions. It is consistent with the binding structure because the two chlorobenzene parts of the ligand seem to interact with the protein hydrophobic pocket by visual inspection. It is also consistent with the fact that many pharmaceutical ligands are considered to gain the binding affinity by vdW interactions. The predicted binding free energy -11.39 kcal/mol is close to the experimental value -12.30 kcal/mol. We estimated the error bars by simply dividing each trajectory data into 10 blocks and calculating the standard deviation of the free energy values

Table 2. Calculation of the Absolute Binding Free Energy of Compound 29 with MDM2 by the Double Decoupling Method^a

	ΔG_{total}	ΔG_{elec}	ΔG_{vdW}	$\Delta G_{\text{restraint}}$
from gas to water	-81.49	-83.51	2.02	0.00
from gas to complex	-92.88	-80.44	-16.92	4.48
from water to complex (binding)	-11.39	3.07	-18.94	4.48

^a $\Delta G_{\text{total}} = \Delta G_{\text{elec}} + \Delta G_{\text{vdW}} + \Delta G_{\text{restraint}}$ for each process. Unit is kcal/mol. Calculated binding free energy is -11.39 kcal/mol, which is comparable with the experimental value -12.30 kcal/mol.

estimated from each block. The error bar was about 0.78 kcal/mol, and thus, the difference between the calculated value and experimental one is reasonably small considering the error bar. Therefore, strong, weak, and non-binders would be distinguished in principle though we need more comprehensive examinations by applying our strategy to many compounds. Because 1.3 and 2.6 kcal/mol roughly correspond to 10 times and 100 times differences in IC₅₀, respectively, we consider that the ability to distinguish at least <2.6 kcal/mol will be necessary for practical applications.

5. CONCLUSIONS

In this article, we proposed a method for first-principles prediction of protein–ligand binding affinity. The method combines the two-dimensional replica-exchange method REUS/REST and double-decoupling method. The advantage of the present method lies in the fact that we do not need to know the protein–ligand binding structures in advance, which

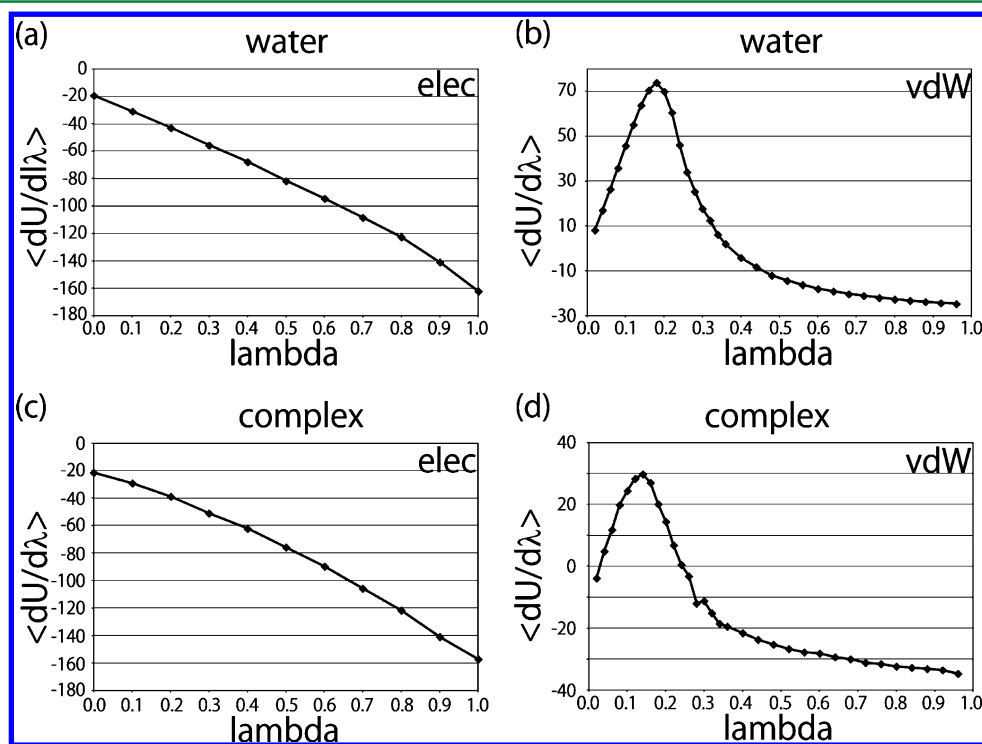


Figure 7. Integrands $\langle \partial U / \partial \lambda \rangle_{\lambda}$ for (a) the electrostatic free energy calculation of the process from gas to water, (b) the vdW free energy calculation of the process from gas to water, (c) the electrostatic free energy calculation of the process from gas to complex, and (d) the vdW free energy calculation of the process from gas to complex as functions of λ . In Thermodynamic Integration method, integrating $\langle \partial U / \partial \lambda \rangle_{\lambda}$ with respect to λ from 0 to 1 gives the free energy difference of the process. The unit is in kcal/mol.

is required by a simple application of the double-decoupling method.

We showed the effectiveness of the scheme from the binding mode predictions to the binding free energy calculations, by applying it to a small protein–ligand system. The method will be very useful for the lead optimization in drug design.

AUTHOR INFORMATION

Corresponding Author

*Email: okamoto@phys.nagoya-u.ac.jp.

Author Contributions

[#]Y.O. and H.K. contributed equally.

Notes

The authors declare no competing financial interest.

ACKNOWLEDGMENTS

The simulations were carried out on the TSUBAME Grid Cluster at the Tokyo Institute of Technology, which was supported by the MEXT Open Advanced Research Facilities Initiative. Y.O. was supported, in part, by the collaboration funds from Takeda Pharmaceutical Co., Ltd., and JSPS Grants-in-Aid for Scientific Research (A) (No. 25247071), for Scientific Research on Innovative Areas (“Dynamical Ordering and Integrated Functions”), and for Computational Materials Science Initiative from MEXT, Japan.

REFERENCES

- (1) Kirkwood, J. G. *J. Chem. Phys.* **1935**, 3, 300–313.
- (2) Zwanzig, R. W. *J. Chem. Phys.* **1954**, 22, 1420–1426.
- (3) Bennett, C. H. *J. Comput. Phys.* **1976**, 22, 245–268.
- (4) Jorgensen, W. L. *Acc. Chem. Res.* **1989**, 22, 184–189.
- (5) Gilson, M. K.; Given, J. A.; Bush, B. L.; McCammon, J. A. *Biophys. J.* **1997**, 72, 1047–1069.
- (6) Jarzynski, C. *Phys. Rev. Lett.* **1997**, 78, 2690–2693.
- (7) Shirts, M. R.; Pitera, J. W.; Swope, W. C.; Pande, V. S. *J. Chem. Phys.* **2003**, 119, 5740–5761.
- (8) Woo, H.-J.; Roux, B. *Proc. Natl. Acad. Sci. U.S.A.* **2005**, 102, 6825–6830.
- (9) Mobley, D. L.; Chodera, J. D.; Dill, K. A. *J. Chem. Phys.* **2006**, 125, 084902–16.
- (10) Gallicchio, E.; Lapelosa, M.; Levy, R. M. *J. Chem. Theory Comput.* **2010**, 6, 2961–2977.
- (11) Gumbart, J. C.; Roux, B.; Chipot, C. *J. Chem. Theory Comput.* **2013**, 9, 794–802.
- (12) Jones, G.; Willett, P.; Glen, R. C.; Leach, A. R.; Taylor, R. J. *Mol. Biol.* **1997**, 267, 727–748.
- (13) Kokubo, H.; Tanaka, T.; Okamoto, Y. *J. Comput. Chem.* **2011**, 32, 2810–2821.
- (14) Kokubo, H.; Tanaka, T.; Okamoto, Y. *J. Chem. Theory Comput.* **2013**, 9, 4660–4671.
- (15) Sugita, Y.; Kitao, A.; Okamoto, Y. *J. Chem. Phys.* **2000**, 113, 6042–6051.
- (16) Kokubo, H.; Tanaka, T.; Okamoto, Y. *J. Comput. Chem.* **2013**, 34, 2601–2614.
- (17) Liu, P.; Kim, B.; Friesner, R. A.; Berne, B. J. *Proc. Natl. Acad. Sci. U.S.A.* **2005**, 102, 13749–13754.
- (18) Berman, H. M.; Westbrook, J.; Feng, Z.; Gilliland, G.; Bhat, T. N.; Weissig, H.; Shindyalov, I. N.; Bourne, P. E. *Nucleic Acids Res.* **2000**, 28, 235–242.
- (19) Okamoto, Y.; Tanaka, T.; Kokubo, H. *J. Comput.-Aided Mol. Des.* **2010**, 24, 699–712.
- (20) Kumar, S.; Rosenberg, J. M.; Bouzida, D.; Swendsen, R. H.; Kollman, P. A. *J. Comput. Chem.* **1992**, 13, 1011–1021.
- (21) Shirts, M. R.; Chodera, J. D. *J. Chem. Phys.* **2008**, 129, 124105.
- (22) Teeter, M. M.; Case, D. A. *J. Phys. Chem.* **1990**, 94, 8091–8097.
- (23) Kitao, A.; Hirata, F.; Go, N. *Chem. Phys.* **1991**, 158, 447–472.
- (24) Garcia, A. E. *Phys. Rev. Lett.* **1992**, 68, 2696–2699.
- (25) Abagyan, R.; Argos, P. *J. Mol. Biol.* **1992**, 225, 519–532.
- (26) Amadei, A.; Linssen, A. B. M.; Berendsen, H. J. C. *Proteins* **1993**, 17, 412–425.
- (27) Kitao, A.; Go, N. *Curr. Opin. Struct. Biol.* **1999**, 9, 164–169.
- (28) Bayly, C. I.; Cieplak, P.; Cornell, W.; Kollman, P. A. *J. Phys. Chem.* **1993**, 97, 10269–10280.
- (29) Cieplak, P.; Cornell, W. D.; Bayly, C.; Kollman, P. A. *J. Comput. Chem.* **1995**, 16, 1357–1377.
- (30) Hornak, V.; Abel, R.; Okur, A.; Strockbine, B.; Roitberg, A.; Simmerling, C. *Proteins* **2006**, 65, 712–725.
- (31) Jorgensen, W. L.; Chandrasekhar, J.; Madura, J. D.; Impey, R. W.; Klein, M. L. *J. Chem. Phys.* **1983**, 79, 926–935.
- (32) Rocklin, G. J.; Mobley, D. L.; Dill, K. A.; Hünenberger, P. H. *J. Chem. Phys.* **2013**, 139, 184103.
- (33) Reif, M. M.; Oostenbrink, C. *J. Comput. Chem.* **2014**, 35, 227–243.
- (34) Darden, T.; York, D.; Pedersen, L. *J. Chem. Phys.* **1993**, 98, 10089–10092.
- (35) Berendsen, H. J. C.; Postma, J. P. M.; van Gunsteren, W. F.; DiNola, A.; Haak, J. R. *J. Chem. Phys.* **1984**, 81, 3684–3690.
- (36) Ryckaert, J.; Ciccotti, G.; Berendsen, H. J. C. *J. Comput. Phys.* **1977**, 23, 327–341.
- (37) Kokubo, H.; Hu, C. Y.; Pettitt, B. M. *J. Am. Chem. Soc.* **2011**, 133, 1849–1858.